DALTON
FULL PAPER

Diastereomeric discrimination in 1,4,7-tris((*S*)-2-hydroxypropyl)-1,4,7-triazacyclononane and its lithium(I), sodium(I) and zinc(II) complexes

Jennifer M. Weeks,[a] Mark A. Buntine,[a] Stephen F. Lincoln,*[a] Edward R. T. Tiekink[a] and Kevin P. Wainwright[b]

[a] *Department of Chemistry, University of Adelaide, Adelaide, SA 5005, Australia. E-mail: Stephen.Lincoln@adelaide.edu.au*
[b] *Department of Chemistry, The Flinders University of South Australia, GPO Box 2100, Adelaide, SA 5001, Australia*

Received 27th October 2000, Accepted 22nd May 2001
First published as an Advance Article on the web 3rd July 2001

In methanol, interchange between equivalent forms of a single diastereomer of 1,4,7-tris((*S*)-2-hydroxypropyl)-1,4,7-triazacyclononanelithium(I), $[Li(S\text{-thpc9})]^+$, and a similar interchange in $[Na(S\text{-thpc9})]^+$ have been characterised by variable temperature $^{13}C\{^1H\}$ NMR spectroscopy. The respective kinetic parameters are: $k = 33.5 \pm 0.8$ and $3030 \pm 80\ s^{-1}$ at 298.2 K, $\Delta H^{\ddagger} = 50.6 \pm 1.0$ and 50.9 ± 1.3 kJ mol^{-1}, and $\Delta S^{\ddagger} = -46.1 \pm 3.4$ and -7.6 ± 4.7 J K^{-1} mol^{-1}, with the corresponding $\log(K/dm^3\ mol^{-1}) = 3.39 \pm 0.05$ and 2.50 ± 0.05 at 298.2 K and $I = 0.05$ mol dm^{-3} (NEt_4ClO_4), where K is the complex stability constant. In *N*,*N*-dimethylformamide (DMF), $\log(K/dm^3\ mol^{-1}) =$ 3.29, 2.29, 2.28, 2.27, 2.29 and 7.59 (all ± 0.05) for $[M(S\text{-thpc9})]^+$ where $M^+ = Li^+$, Na^+, K^+, Rb^+, Cs^+ and Ag^+, respectively. For the interchange between equivalent forms of a single diastereomer of 1,4,7-tris((*S*)-2-hydroxy-2-phenylethyl)-1,4,7-triazacyclononanelithium(I), $[Li(S\text{-thpec9})]^+$, and a similar interchange in $[Na(S\text{-thpec9})]^+$, the kinetic parameters obtained in DMF are: $k = 20.5 \pm 0.8$ and $k = 8600 \pm 200\ s^{-1}$ at 298.2 K, $\Delta H^{\ddagger} = 32.8 \pm 1.8$ and 54.7 ± 1.2 kJ mol^{-1}, and $\Delta S^{\ddagger} = -110 \pm 3.2$ and 13.8 ± 4.2 J K^{-1} mol^{-1}, respectively. In DMF, $\log(K/dm^3\ mol^{-1}) = 3.64$, 2.03, 1.91, 1.91, 1.62 and 7.59 (all ± 0.05) for $[M(S\text{-thpc9})]^+$ where $M^+ = Li^+$, Na^+, K^+, Rb^+, Cs^+ and Ag^+, respectively. Gas phase *ab initio* modelling shows *S*-thpc9, *S*-thpec9 and their Li^+, Na^+ and Zn(II) complexes to assume single distorted trigonal prismatic diastereomeric conformations, as do X-ray crystallographic, *ab initio* modelling and $^{13}C\{^1H\}$ NMR spectroscopic solution studies of $[Zn(S\text{-thpc9})]^+$.

Introduction

Pendant arm polyaaza macrocyclic complexes have attracted attention because of their intrinsic interest[1–10] and also because of their potential use as biological tracers,[11,12] in ion specific electrodes[13] and in solvent extraction.[14] Their use as magnetic resonance imaging contrast agents in the case of some lanthanide(III) complexes is widespread.[15–20] When each pendant arm incorporates the same chiral centre one diastereomer of both the ligand and its metal complexes may be dominantly stable as has been reported for 1,4,7,10-tetrakis((*R*)-2-hydroxypropyl)- and 1,4,7,10-tetrakis((*R*)-2-hydroxy-2-phenylethyl)-1,4,7,10-tetraazacyclododecane and their alkali metal complexes.[21,22] Such chiral discrimination between diastereomers in a free octadentate ligand and its eight-coordinate metal complexes in solution is unusual, and it is of interest to know to what extent this phenomenon extends to ligands and metal complexes of other denticities and coordination numbers.

Accordingly, we now report a study of the alkali metal complexes of hexadentate 1,4,7-tris((*S*)-2-hydroxypropyl)- and 1,4,7-tris((*S*)-2-hydroxy-2-phenylethyl)-1,4,7-triazacyclononane, *S*-thpc9 and *S*-thpec9, where each arm of either ligand incorporates a (*S*) chiral centre. We find that both ligands complex Li^+ in preference to the other alkali metal ions in methanol and *N*,*N*-dimethylformamide, DMF. Our ^{13}C NMR and *ab initio* modelling studies are consistent with $[Li(S\text{-thpc9})]^+$ and its Na^+ analogue and $[Li(S\text{-thpc9})]^+$ and its Na^+ analogue existing as single diastereomers interchanging rapidly between two equivalent forms in methanol and DMF, respectively. Such interchanges are shown schematically in Fig. 1a, and are compared with the rapid enantiomerisation of Δ- and Λ-1,4,7-tris(2-hydroxyethyl)-1,4,7-triazacyclononanelithium(I), Δ and Λ$[Li(thec9)]^+$, and its Na^+ analogue shown schematically in Fig. 1b.[9] ^{13}C NMR solution studies and *ab initio* of $[Zn(S\text{-thpc9})]^+$ and $[Zn(S\text{-thpec9})]^+$ are also consistent with the dominance of one diastereomer, as is an X-ray crystallographic study of $[Zn(S\text{-thpc9})]^+$.

Results and discussion

Complex stability

The stability constants for the alkali metal complexes of thec9, *S*-thpc9 and *S*-thpec9 in methanol and DMF are collected in Table 1 from which it is seen that thec9 is weakly selective for Na^+ while *S*-thpc9 and *S*-thpec9 are selective for Li^+. This change in selectivity is consistent with increasing pendant arm bulk imposing steric restraints on the ligand cavity size such that thec9 more readily accommodates Na^+ while *S*-thpc9 and *S*-thpec9 more readily accommodate Li^+. It is also consistent with the observation that thec9 barely discriminates between coordination of Mg^{2+} and Ca^{2+}, while *S*-thpc9 and *S*-thpec9 both discriminate strongly in coordinating Mg^{2+} in preference to Ca^{2+} in acetonitrile.[8,13] The stabilities of $[Ag(S\text{-thpc9})]^+$, $[Ag(S\text{-thpec9})]^+$ and $[Ag(thec9)]^+$ (Table 1) are high relative to those of their alkali metal analogues. This is attributable to the borderline soft Lewis base amines of these ligands competing with hard Lewis base solvents more effectively for the soft

Table 1 Stability constants for $[M(thec9)]^+$, $[M(S\text{-thpc9})]^+$ and $[M(S\text{-thpec9})]^+$ at 298.2 K and $I = 0.05$ mol dm^{-3} (Et_4NClO_4)

	log(K/dm^3 mol^{-1})					
Ligand/solvent	$M^+ = Li^+$	Na^+	K^+	Rb^+	Cs^+	Ag^+ [a]
thec9/MeOH [b]	3.13	3.52	3.23	2.8	2.47	7.65
S-thpc9/MeOH [c]	3.39	2.50	[d]	[d]	[d]	7.39
S-thpc9/DMF [c]	3.29	2.29	2.28	2.27	2.29	7.59
S-thpec9/DMF [c]	3.64	2.03	1.91	1.91	1.62	7.59

[a] It was necessary to determine Ag^+ complex stability constants to facilitate the competitive titration method used to determine the alkali metal complex stability constants. [b] Ref. 9. [c] Single standard deviations in log(K/dm^3 mol^{-1}) did not exceed ±0.05 in any case. [d] Insufficiently soluble for stability constant determination.

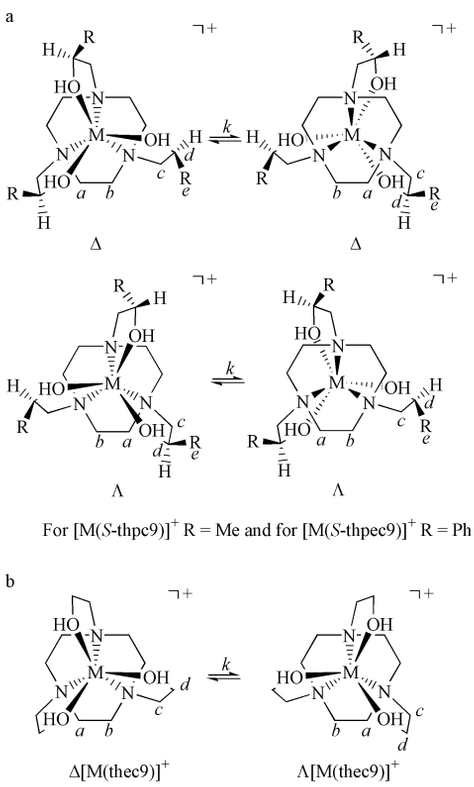

Fig. 1 (a) Interchange between two equivalent forms of either Δ[M(*S*-thpc9)]$^+$ or Δ[M(*S*-thpec9)]$^+$ or Λ[M(*S*-thpc9)]$^+$ or Λ[M(*S*-thpec9)]$^+$. (b) Enantiomerisation of Δ and Λ[M(thec9)]$^+$. The convention adopted assigns Δ and Λ to a structure where the trigonal nitrogen plane is twisted by an angle φ to the right and the left, respectively, by reference to the trigonal oxygen plane when viewed down the C_3 axis. For a trigonal prism $\varphi = 0°$. The φ angles shown are exaggerated for the purposes of illustration.

Lewis acid Ag^+ than for the hard Lewis acid alkali metal ions.[23]

Diastereomer interchange processes

The Δ and Λ diastereomers of $[M(S\text{-thpc9})]^+$ shown in Fig. 1a (R = Me), are characterised by the trigonal nitrogen plane being twisted by an angle φ to the right and left, respectively, by reference to the trigonal oxygen plane when viewed down the C_3 axis. For a trigonal prism $\varphi = 0°$. (In earlier studies we have assigned Δ and Λ in the opposite manner using a different convention.[4,5,9,1,21,22]) In principle, these diastereomers may be interconverted by a single nitrogen inversion at each of the three nitrogens of the macrocycle. Because there is no equivalence between carbon atoms in each of the diastereomers, Δ and Λ$[M(S\text{-thpc9})]^+$ should be characterised by separate ^{13}C NMR spectra each consisting of five resonances arising from the five unique carbons, *a*–*e* and *a*′–*e*′, in each diastereomer.

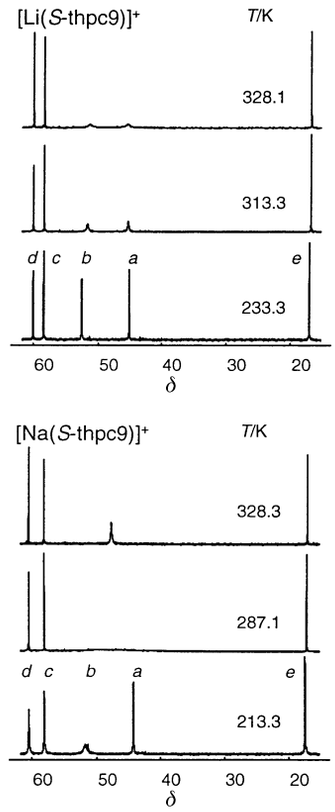

Fig. 2 The temperature variation of the $^{13}C\{^1H\}$ 75.47 MHz NMR spectra of $\Delta[Li(S\text{-thpc9})]^+$ and $\Delta[Na(S\text{-thpc9})]^+$ in ^{12}C enriched [$^2H_4$]methanol arising from solutions 0.10 mol dm^{-3} in $[M^+]_{total}$ and $[S\text{-thpc9}]_{total}$.

However, variable temperature ^{13}C NMR studies show a single five resonance spectrum at low temperature in which the resonances assigned to the CH_2 macrocyclic carbons, *a* and *b*, broaden and coalesce to a singlet for $[Li(S\text{-thpc9})]^+$ and $[Na(S\text{-thpc9})]^+$, respectively, at temperatures just below the ^{12}C enriched [$^2H_4$]methanol solution boiling point as shown in Fig. 2. (The individual CH_2 resonances cannot be assigned to individual macrocyclic carbons on the basis of the available data.) This is consistent with each complex interconverting between equivalent forms of single diastereomers through double inversions at each nitrogen as shown in Fig. 1a. (These appear to be the Δ diastereomers for $[Li(S\text{-thpc9})]^+$ and $[Na(S\text{-thpc9})]^+$ from the *ab initio* modelling discussed below.) The CH_2 macrocyclic carbons, *a* and *b*, interchange environments with increasing rapidity as the temperature increases with a resulting broadening and coalescence of their resonances. Carbons *c*–*e* of CH_2N, $OCHCH_3$ and $OCHCH_3$, respectively, interchange between equivalent environments and show no change in their resonances associated with the interchange process although they show some narrowing as the temperature increases and viscosity decreases.

Each of Δ and $\Lambda[M(S\text{-thpec9})]^+$ should be characterised by separate spectra consisting of four resonances arising from the four unique carbons, *a*–*d*, and a multiplet, *e*, arising from the phenyl groups in each diastereomer (Fig. 1a, R = Ph). However, at low temperature only four resonances *a*–*d*, and one multiplet, *e*, are observed. The resonances assigned to the CH_2 macrocyclic carbons, *a* and *b*, broaden and coalesce to a singlet, respectively, for $[Li(S\text{-thpec9})]^+$ and $[Na(S\text{-thpec9})]^+$ at temperatures just below the ^{12}C enriched [$^2H_7$]DMF solution boiling point as shown in Fig. 3. This is also consistent with each of these complexes interchanging between equivalent forms of single diastereomers through double nitrogen inversions at each nitrogen as shown in Fig. 1a. (*Ab initio* modelling also indicates that $[Li(S\text{-thpec9})]^+$ and $[Na(S\text{-thpec9})]^+$ exist as Δ diastereomers in the gas phase as discussed below.)

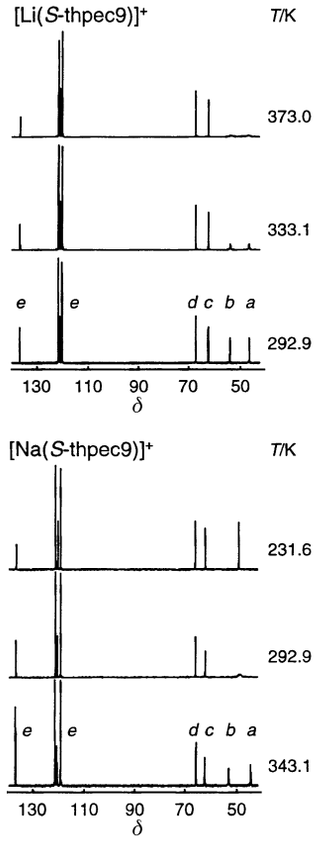

Fig. 3 The temperature variation of the $^{13}C\{^{1}H\}$ 75.47 MHz NMR spectra of $\Delta[Li(S\text{-thpec9})]^+$ and $\Delta[Na(S\text{-thpec9})]^+$ in $[^2H_7]N,N$-dimethylformamide arising from solutions 0.10 mol dm^{-3} in $[M^+]_{total}$ and $[S\text{-thpec9}]_{total}$.

Complete lineshape analyses[24] of the broadening and coalescence of the *a* and *b* ^{13}C resonances arising from the four complexes, as exemplified by $[Na(S\text{-thpc9})]^+$ in Fig. 4, yield the mean lifetimes of the CH_2 macrocyclic carbons *a* and *b* in their different environments, τ, such that:

$$1/\tau = k = k_B T/h \exp(-\Delta H^{\ddagger}/RT + \Delta S^{\ddagger}/R) \qquad (1)$$

where *k* is the rate constant for interconversion between the two equivalent forms of the diastereomers of each of the four complexes. The derived τ values (ms) and the experimental temperatures (K) in brackets are 4.2 (328.1), 5.8 (323.2), 7.8 (318.2), 10.2 (313.3), 15.0 (308.3), 21.5 (303.3), 31.3 (298.4) and 43.1 (292.3) for $[Li(S\text{-thpc9})]^+$; 0.23 (303.4). 0.41 (293.1), 0.93 (287.1), 1.62 (276.8), 2.56 (271.6), 6.60 (261.3), 18.6 (250.9) and 59.5 (240.6) for $[Na(S\text{-thpc9})]^+$; 3.80 (362.9), 4.40 (358.0), 5.23 (353.0), 6.39 (348.1), 7.82 (343.2), 8.63 (338.3) and 10.8 (333.4) for $[Li(S\text{-thpec9})]^+$; and 0.09 (303.3), 0.16 (292.9), 0.42 (281.9), 0.67 (276.8), 1.07 (271.6), 1.91 (266.4), 3.39 (261.3) and 8.25 (250.9) for $[Na(S\text{-thpec9})]^+$. The kinetic parameters calculated from these data through eqn. (1) are collected in Table 2.

Interchanges between the two equivalent forms of the diastereomers of each of $\Delta[Li(S\text{-thpc9})]^+$, $\Delta[Na(S\text{-thpc9})]^+$, $\Delta[Li(S\text{-thpec9})]^+$ and $\Delta[Na(S\text{-thpec9})]^+$ are much slower at 298.2 K than the enantiomerisation of Δ and $\Lambda[Li(thec9)]^+$ and Δ and $\Lambda[Na(thec9)]^+$ largely because of the greater $\Delta H^{\ddagger}$ of the former processes. The enantiomerisation of Δ and $\Lambda[Li(thec9)]^+$ and Δ and $\Lambda[Na(thec9)]^+$ may be achieved through a trigonal twist mechanism involving a single inversion at each nitrogen without displacement of the metal centre from between the trigonal oxygen and nitrogen planes of thec9 (Fig. 1b). In contrast, the interchange processes for $\Delta[Li(S\text{-thpc9})]^+$, $\Delta[Na(S\text{-thpc9})]^+$, $\Delta[Li(S\text{-thpec9})]^+$ and $\Delta[Na(S\text{-thpec9})]^+$ require the translation of the trigonal oxygen plane and metal centre from one side of the trigonal nitrogen plane to the other as seen in Fig. 1a. Both Li^+ and Na^+ are too large to pass through the centre of the trigonal nitrogen planes of *S*-thpc9 and *S*-thpec9, and the double inversion at each nitrogen consequently requires the detachment of the metal centre from each of the three hydroxy coordinating groups and reattachment at some stage in the interchange process. Although the rate determining step is unknown, the relative slowness of the interchange processes for $\Delta[Li(S\text{-thpc9})]^+$, $\Delta[Na(S\text{-thpc9})]^+$, $\Delta[Li(S\text{-thpec9})]^+$ and $\Delta[Na(S\text{-thpec9})]^+$ at 298.2 K relates to the requirement for a double nitrogen inversion to occur at each nitrogen, whereas for the enantiomerisation of Δ and $\Lambda[Li(thec9)]^+$ and Δ and $\Lambda[Na(thec9)]^+$ only a single nitrogen inversion and no bond breaking or making is required.

The $[K(S\text{-thpc9})]^+$ and $[K(S\text{-thpec9})]^+$ macrocyclic ring carbon resonances also coalesce to a singlet as the temperature

Table 2 Kinetic parameters for $[M(thec9)]^+$ and $\Delta[M(S\text{-thpc9})]^+$ in ^{12}C enriched $[^2H_4]$methanol, and $\Delta[M(S\text{-thpec9})]^+$ in $[^2H_7]N,N$-dimethylformamide

Complex	k (298.2 K)/ s^{-1}	$\Delta H^{\ddagger}$/ kJ mol^{-1}	$\Delta S^{\ddagger}$/ J K^{-1} mol^{-1}
$[Li(thec9)]^+$ [a]	1.11×10^6	27.2	−36.3
$[Na(thec9)]^+$ [a]	2.27×10^5	21.7	−69.6
$\Delta[Li(S\text{-thpc9})]^+$	33.5 ± 0.8	50.6 ± 1.0	−46.1 ± 3.4
$\Delta[Na(S\text{-thpc9})]^+$	3030 ± 80	50.9 ± 1.3	−7.6 ± 4.7
$\Delta[Li(S\text{-thpec9})]^+$	20.5 ± 0.8	32.8 ± 1.8	−110 ± 3.2
$\Delta[Na(S\text{-thpec9})]^+$	8600 ± 200	54.7 ± 1.2	13.8 ± 4.2

[a] Ref. 9.

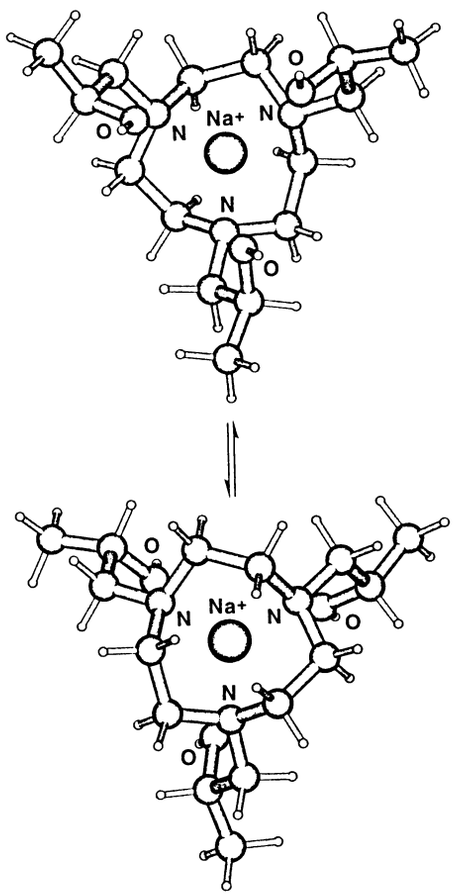

Fig. 4 Global energy minimised *ab initio* modelled structures of equivalent forms of $\Delta[Na(S\text{-thpc9})]^+$ viewed down the C_3 axes from the trigonal oxygen plane and illustrating the diastereomeric interchange process. Bonds between Na^+ (the atom on the C_3 axis) and *S*-thpc9 are omitted for clarity.

Table 3 Dimensions from gas phase *ab initio* modelling through Gaussian 94 using the HF/LanL2DZ basis set

Dimension	*S*-thpc9	Li(*S*-thpc9)]$^+$	Na(*S*-thpc9)]$^+$	[K(*S*-thpc9)]$^+$
φ/°	−39.2	14.2	9.9	9.5
O–O/Å	3.11	2.97	3.72	4.59
N–N/Å	4.82	2.94	3.03	3.10
O_{plane}–N_{plane}/Å	2.57	2.71	2.83	2.82
M–O_{plane}/Å	—	1.16	0.95	0.53
M–N_{plane}/Å	—	1.55	1.88	2.29
	S-thpec9	[Li(*S*-thpec9)]$^+$	[Na(*S*-thpec9)]$^+$	[K(*S*-thpec9)]$^+$
φ/°	−34.0	13.7	7.9	9.1
O–O/Å	4.41	3.02	3.71	4.60
N–N/Å	3.10	2.94	3.03	3.11
O_{plane}–N_{plane}/Å	2.93	2.72	2.84	2.81
M–O_{plane}/Å	—	1.15	0.96	0.52
M–N_{plane}/Å	—	1.57	1.88	2.29

increases consistent with an exchange process occurring similar to that seen in their lighter analogues. However, the pendant arm carbon resonances are substantially broadened at low temperature in both cases. This may indicate that [K(*S*-thpc9)]$^+$ and [K(*S*-thpec9)]$^+$ exist in equilibrium with [K(*S*-thpc9)-(MeOH)$_n$]$^+$ and [K(*S*-thpc9)(MeOH)$_n$]$^+$, respectively, where K^+ increases its coordination number beyond 6, and interchange occurs between species of different coordination numbers. As a consequence, quantitative variable temperature ^{13}C NMR studies were not undertaken. The solubilities of $RbCF_3SO_3$ and $CsCF_3SO_3$ in methanol at low temperature are insufficient for quantitative ^{13}C NMR studies of [Rb(*S*-thpc9)]$^+$ and [Cs(*S*-thpc9)]$^+$.

In methanol *S*-thpec9 shows sharp ^{13}C *c*–*e* resonances and two broad *a* and *b* resonances at temperatures just above the solution freezing point consistent with the macrocyclic carbons *a* and *b* entering the slow regime of the NMR timescale. Gas phase *ab initio* modelling shows *S*-thpec9 to adopt a distorted trigonal prismatic stereochemistry similar to that shown for Δ[M(*S*-thpec9)]$^+$ in Fig. 1a except that the Λ diastereomer appears to be the more stable, as is discussed below. The broad ^{13}C NMR doublet observed for the *S*-thpec9 *a* and *b* carbons is consistent with interchange occurring between equivalent forms of its Λ diastereomer in an analogous manner to that proposed for the interchange observed for Δ[Li(*S*-thpec9)]$^+$. No resolution into a doublet of the *a* and *b* ^{13}C resonances of *S*-thpc9 is observed in methanol at low temperature consistent with interchange of the macrocyclic carbons *a* and *b* between different environments being in the fast regime of the NMR timescale. The tetraaza analogues of *S*-thpc9 and *S*-thpec9, 1,4,7,10-tetrakis((*R*)-2-hydroxypropyl)- and 1,4,7,10-tetrakis((*R*)-2-hydroxy-2-phenylethyl)-1,4,7,10-tetraazacyclododecane, both exhibit separate ^{13}C resonances for their macrocyclic *a* and *b* carbons consistent with the presence of a single diastereomer in each case.[21,22]

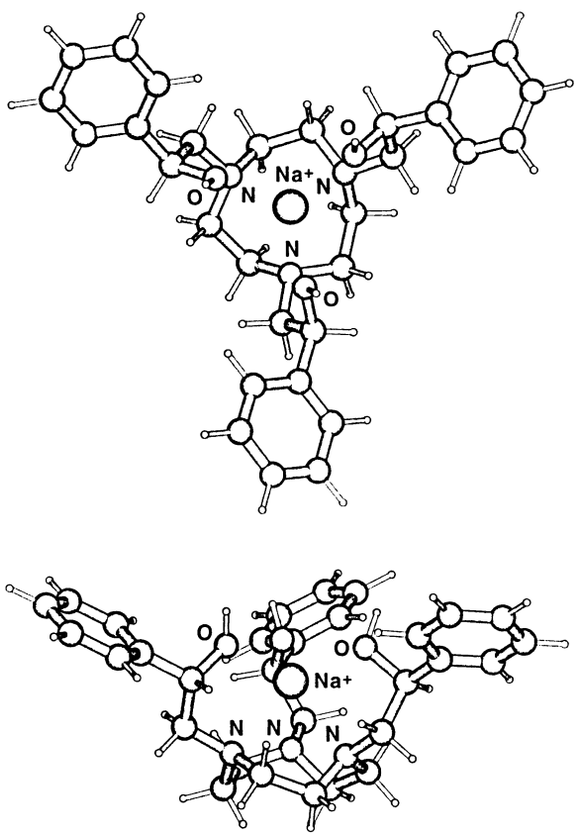

Fig. 5 Global energy minimised *ab initio* modelled structures of Δ[Na(*S*-thpec9)]$^+$ viewed down the C_3 axes from the three oxygen plane (above) and viewed from the side (below).

Ab initio modelling

While the NMR data is consistent with the complexes existing as single diastereomers, they do not permit diastereomer identification. Accordingly, the complexes were modelled primarily to gain insight into the probable identity of the diastereomers. Selected dimensions for Λ*S*-thpc9, Δ[Li(*S*-thpc9)]$^+$ and its Na^+ and K^+ analogues, and Λ*S*-thpec9, Δ[Li(*S*-thpec9)]$^+$ and its Na^+ and K^+ analogues obtained from gas phase *ab initio* modelling through Gaussian 94 using the HF/LanL2DZ basis set[25] are shown in Table 3. In each case the parallel trigonal oxygen and nitrogen planes define opposing faces of a distorted trigonal prism. When viewed down the C_3 axis from the oxygen plane, the nitrogen plane is twisted to the left from trigonal prismatic stereochemistry in Λ*S*-thpc9 and its twist angle, φ, is defined as negative. However, the nitrogen plane is twisted to the right in Δ[Li(*S*-thpc9)]$^+$ and its Na^+ and K^+ analogues and their φ are defined as positive and their overall chirality as Δ (Table 3). The modelled structure of Δ[Na(*S*-thpc9)]$^+$ is shown in its two equivalent forms in Fig. 4 which are consistent with the interpretation of the observed ^{13}C NMR spectral temperature variation. When proceeding from the nitrogen atom in a clockwise manner, the adjacent macrocyclic methylene carbon is below the second methylene carbon in a repeating "down-up" sequence around the macrocyclic ring of Λ*S*-thpc9 and its Δ complexes, as is also the case for Λ*S*-thpec9 and its Δ complexes. For Λ*S*-thpec9, φ is negative while it is positive for Δ[Li-(*S*-thpec9)]$^+$ and its Na^+ and K^+ analogues (Table 3 and Fig. 5). The change from methyl to phenyl substitution at the α carbons of the ligands has little effect on the distortion of the coordinating atom set from trigonal prismatic geometry compared with the effect of the coordination of Li^+, Na^+ and K^+ which

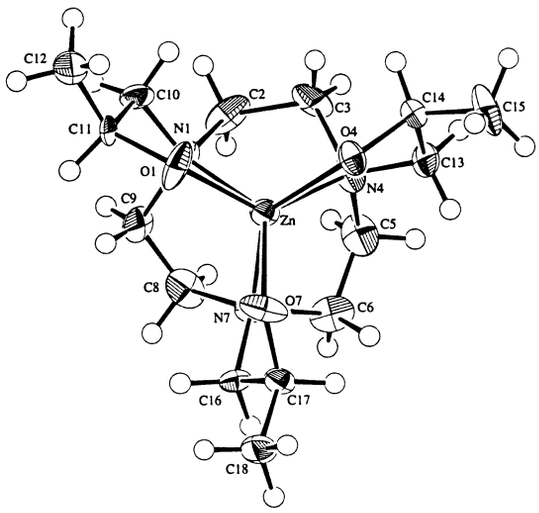

Fig. 6 Molecular structure and crystallographic numbering scheme employed for the Δ[Zn(*S*-thpc9)]$^{2+}$ cation.

changes the sign of φ. (The other diastereomers of *S*-thpc9, *S*-thpec9 and their Li^+, Na^+ and K^+ complexes may be obtained through single inversions at each nitrogen (Fig. 1a) but they are of higher energy and represent local energy minimum structures.) The separation between the trigonal oxygen and nitrogen planes of *S*-thpc9 is significantly less than that of *S*-thpec9 which probably reflects the greater bulk of the phenyl groups of the latter. As the size of M^+ increases in [M(*S*-thpc9)]$^+$ and [M(*S*-thpec9)]$^+$ so it moves away from the trigonal nitrogen plane and towards the trigonal oxygen plane and the separation between the two planes changes as is seen for the Li^+, Na^+ and K^+ complexes in Table 3. This suggests that K^+ may be more exposed to solvent interaction which may explain some of the variations of the solution NMR spectra of [K(*S*-thpc9)]$^+$ and [K(*S*-thpec9)]$^+$ discussed above. It is seen that for both of the free ligands and their complexes, distorted trigonal prismatic stereochemistry is preferred. However, the Λ and Δ diastereomers are the most stable for the free ligands and their complexes, respectively. This change in chirality probably reflects the competition between steric effects in the ligand and the alkali metal to donor atom bond length requirements of the complexes.

X-Ray crystallography, *ab initio* modelling and ^{13}C NMR spectroscopy of [Zn(*S*-thpc9)]$^{2+}$

The X-ray crystallographically determined structure of [Zn(*S*-thpc9)]$^{2+}$ shows the parallel trigonal oxygen and nitrogen *S*-thpc9 planes to be slightly staggered by 7.3° which constitutes the twist angle, φ, of the approximately trigonal prismatic six-coordinate zinc(II) environment shown in Fig. 6. (The twist angle of a trigonal prism is defined as 0°.) Selected bond angles and distances appear in Table 4. A selection of distances and the φ values determined by X-ray crystallography and calculated by *ab intio* calculations appear in Table 5, from which it is apparent that both structures for [Zn(*S*-thpc9)]$^+$ are in broad agreement. The sign of φ is positive in both cases consistent with the Δ diastereomer. The Δ diastereomer of [Zn(*S*-thpc9)]$^{2+}$ was also observed in the X-ray crystallographically determined dimer structure formed by [Zn(*S*-thpc9)]$^{2+}$ and [V(*S*-thpc9′)]$^+$, where in [*S*-thpc9′]$^{3-}$ each of the hydroxy groups of *S*-thpc9 are deprotonated.[3] In this case, φ decreased to 4.5° consistent with small changes in the various forces affecting structure in the crystalline state being reflected in a change in φ. On this basis some minor differences in structural dimensions between the crystallographically determined [Zn(*S*-thpc9)]$^{2+}$ structure and that calculated by *ab initio* methods are expected. These observations indicate that *ab initio* calculations give a reasonable guide to the chirality of [Zn(*S*-thpc9)]$^{2+}$, and probably to that of its Li^+ and Na^+ analogues and *S*-thpc9 also. A similar assumption is made for *S*-thpec9 and its complexes. Trigonal prismatic Zn^{2+} complexes are unusual, and it appears that the stereochemical constraint induced by incorporation of the three nitrogen donor atoms into the macrocylic structure together with the steric requirements of the three pendant arms are largely responsible for this stereochemistry.

In [$^2H_4$]methanol at 298.2 K, [Zn(*S*-thpc9)]$^{2+}$ exhibited five $^{13}C\{^1H\}$ resonances corresponding to the inequivalent macrocyclic CH_2 carbons at 50.43 and 57.10 ppm (but which cannot be separately assigned on the basis of these data) and the pendant arm NCH_2, CH and CH_3 carbons at 65.60, 65.31 and 20.10 ppm, respectively, corresponding to *a*–*e* in Fig. 1a. Thus, [Zn(*S*-thpc9)]$^{2+}$ exists as a single diastereomer (assigned the Δ configuration on the basis of the X-ray crystallographic data and *ab initio* calculations) in undergoing slow interchange as shown in Fig. 1a. This slowness of interchange relative to that of [Li(*S*-thpc9)]$^+$ and [Na(*S*-thpc9)]$^+$ is attributed to the higher surface charge density of Zn^{2+} and stronger interaction with the donor atoms by comparison with that of the alkali metal ions. A similar slowness of intramolecular exchange, attributed to the same cause, was observed for Δ[Zn(*S*-thpec9)]$^{2+}$ in [$^2H_7$]*N*,*N*-dimethylformamide at 298.2 K.

Table 4 Selected bond lengths (Å) and angles (°) for the Δ[Zn(*S*-thpc9)]$^{2+}$ cation

Zn–O1	2.167(5)	Zn–O4	2.110(5)
Zn–O7	2.118(5)	Zn–N1	2.128(4)
Zn–N4	2.168(6)	Zn–N7	2.175(5)
O1–Zn–O4	87.8(2)	O1–Zn–O7	82.6(2)
O1–Zn–N1	78.6(2)	O1–Zn–N4	141.0(2)
O1–Zn–N7	128.1(2)	O4–Zn–O7	89.0(2)
O4–Zn–N1	127.5(2)	O4–Zn–N4	78.1(2)
O4–Zn–N7	140.0(2)	O7–Zn–N1	137.6(2)
O7–Zn–N4	132.5(2)	O7–Zn–N7	80.2(2)
N1–Zn–N4	81.6(2)	N1–Zn–N7	82.1(2)
N4–Zn–N7	81.3(2)	Zn–O1–C11	114.5(4)
Zn–O4–C14	117.2(4)	Zn–O7–C17	110.9(4)
Zn–N1–C2	111.0(4)	Zn–N1–C9	102.4(4)
Zn–N1–C10	108.9(4)	Zn–N4–C3	102.7(4)
Zn–N4–C5	109.9(4)	Zn–N4–C13	108.2(4)
Zn–N7–C6	104.2(4)	Zn–N7–C8	107.4(4)
Zn–N7–C16	107.3(4)		

Table 5 Dimensions for Δ[Zn(*S*-thpc9)]$^{2+}$ determined by X-ray crystallography and calculated by *ab initio* modelling through Gaussian 94 using the HF/LanL2DZ basis set

Dimension	By X-ray	By modelling
φ/°	−7.3	−19.1
O–O/Å	2.93	3.05
N–N/Å	2.83	2.90
O_{plane}–N_{plane}/Å	2.73	2.64
Zn–O_{plane}/Å	1.31	1.19
Zn–N_{plane}/Å	1.42	1.45

Conclusion

This study shows that the sexadentate pendant arm ligands 1,4,7-tris((*S*)-2-hydroxypropyl)-1,4,7-triazacyclononane, *S*-thpc9, and 1,4,7-tris((*S*)-2-hydroxy-2-phenylethyl)-1,4,7-triazacyclononane, *S*-thpec9, preferentially coordinate Li^+ of the alkali metal ions in DMF and that both coordinate Zn^{2+}. In DMF, [Li(*S*-thpc9)]$^+$, [Na(*S*-thpc9)]$^+$, [Li(*S*-thpec9)]$^+$, and [Na(*S*-thpec9)]$^+$ exist as single diastereomers which interconvert between equivalent forms at rates within the ^1H (300 MHz) timescale. In contrast, the analogous interconversions of [Zn(*S*-thpc9)]$^+$ and [Zn(*S*-thepc9)]$^+$, which also exist as single diastereomers, are slow on the ^1H NMR timescale in methanol.

Crystallographic studies show that $[Zn(S\text{-thpc9})]^+$ possesses a distorted trigonal prismatic structure where Zn^{2+} lies between parallel, trigonal oxygen and trigonal nitrogen donor atom planes in a Δ configuration. This provided an opportunity to assess the validity of using *ab initio* modelling to gain insight into the distereomers for which experimentally determined structures were unavailable. It showed $[Zn(S\text{-thpc9})]^+$ to exist as a single Δ diastereomer with a distorted trigonal prismatic structure broadly similar to that observed in the solid state. It also showed the four alkali metal complexes to exist as single distorted trigonal prismatic diastereomers with Δ configurations, from which it is deduced that similar structures exist for the single diastereomers observed in solution.

Experimental

Syntheses

1,4,7-Tris((*S*)-2-hydroxypropyl)-1,4,7-triazacyclononane. Synthesis was achieved through elaboration of 1,4,7-triazacyclononane (tacn) prepared as described in the literature.[26] *S*-(−)-Propylene oxide (0.116 g, 0.002 mol) was added to a solution of triazacyclononane (0.079 g, 0.0006 mol) in ethanol (10 cm^3) and left to stir at room temperature overnight. The solution was then evaporated to dryness at reduced pressure and the product was obtained as a colourless oil in quantitative yield. ^{13}C NMR in $CDCl_3$: δ 66.4, 63.4, 52.7, 19.8 (Found: C, 55.78; H, 10.35; N, 13.30. $C_{15}H_{30}N_3O_3 \cdot 1.25H_2O$ requires C, 55.79; H, 10.14; N, 13.01%). A preparation of this ligand from tacn·3HBr has been reported.[1]

1,4,7-Tris((*S*)-2-hydroxy-2-phenylethyl)-1,4,7-triazacyclononane. *S*-(−)-Styrene oxide (0.25 g, 0.002 mol) was added to a solution of triazacyclononane (0.079 g, 0.0006 mol) in DMF (10 cm^3) and was left to stir at 85 °C for three days. Upon cooling to room temperature, methanol (5 cm^3) and water (5 cm^3) were added resulting in the formation of a fine white precipitate which was filtered off, washed with water and dried under vacuum. Yield 0.261 g, 89%. ^{13}C NMR in $CDCl_3$: δ 142.5, 128.3, 127.3, 126.0, 70.7, 67.9, 53.7 (Found: C, 73.49; H, 8.05, N, 8.56. $C_{30}H_{39}O_3N_3$ requires C, 73.62; H, 7.98; N, 8.59%). A similar preparation is reported in the literature.[8,12]

$[Zn(S\text{-thpc9})][ClO_4]_{1.5}Cl_{0.5}$. Crystals were obtained by the slow evaporation of an equimolar aqueous solution of $Zn(ClO_4)_2$ and *S*-thpc9 at ambient temperature. The origin of chloride in the crystal is unclear.

Physical methods

^{12}C Enriched $[^2H_4]$methanol (99.5% ^{12}C and 99.5% ^2H, Aldrich) was dried over 3 Å molecular sieves prior to use in preparation of NMR samples. Analytical grade methanol (BDH Analar) and spectroscopic grade DMF (Aldrich) were used in the preparation of samples for potentiometric titration. In both cases, the water content was below the 50 ppm detection level of the Karl–Fischer method. $^{13}C\{^1H\}$ NMR spectra (75.47 MHz) were run on a Varian Gemini 300 spectrometer. Samples were thermostatted to within ± 0.3 K. The stability constants for $[M(S\text{-thpc9})]^+$ were potentiometrically determined in triplicate by a literature method.[27] Lineshape analyses[24] and *ab initio* modelling[24] were performed on a Digital Venturis 575 computer and a Silicon Graphics Indigo^2 work station, respectively. The *ab initio* modelling incorporated all electrons for H, C, N and O, and the valence electrons for Li^+, Na^+ and Zn^{2+} together with their effective core potentials.[28] To check that the modelled structures in Fig. 4 and 5 and their analogues represent those with minimum global energies, two basic structures with either three or two pendant arms on the same side of the three nitrogen plane were used as starting points. A range of macrocyclic ring and pendant arm conformations were then superimposed on these structures to give a broad selection of starting points. In each case the energy minimised structures obtained were those characterised by the dimensions shown in Table 3 and depicted in Fig. 4 and 5 consistent with global energy minima being reached in each case.

Crystal structure determination of $[Zn(S\text{-thpc9})][ClO_4]_{1.5}Cl_{0.5}$

Crystal data. $C_{15}H_{33}Cl_2N_3O_9Zn$, $M = 535.7$, monoclinc, $a = 17.6183(6)$, $b = 10.4941(2)$, $c = 14.4786(5)$ Å, $\beta = 123.504(1)°$, $T = 173$ K, space group $C2$, $Z = 4$, μ(Mo-Kα) = 13.91 cm^{-1}, 17857 reflections measured on a Nonius Kappa CCD, θ_{max} 30.0°, 7443 unique ($R_{int} = 0.055$), 4797 with $I \geq 3.0\sigma(I)$ were used in subsequent calculations: final $R = 0.065$ and $R_w = 0.075$.[29] The absolute structure was determined on the basis of the known chirality of the (*S*)-2-hydroxypropyl pendant arms. The O–*H* atoms were not located.

CCDC reference number 164174.

See http://www.rsc.org/suppdata/dt/b0/b008687h/ for crystallographic data in CIF or other electronic format.

Acknowledgements

Funding by the Australian Research Council and the University of Adelaide, and the award of a University of Adelaide Research Scholarship to J. M. W. are gratefully acknowledged.

References

1 J. Robb and R. D. Peacock, *Inorg. Chim. Acta*, 1986, **121**, L15.
2 A. A. Belal, L. J. Farrugia, R. D. Peacock and J. Robb, *J. Chem. Soc.*, *Dalton Trans.*, 1989, 931.
3 I. Fallis, J. Farrugia, N. M. Macdonald and R. D. Peacock, *Inorg. Chem.*, 1993, **32**, 779.
4 S. L. Whitbread, S. Politis, A. K. W Stephens, J. B. Lucas, R. Dhillon, S. F. Lincoln and K. P. Wainwright, *J. Chem. Soc.*, *Dalton Trans.*, 1996, 1379.
5 A. K. W. Stephens, R. Dhillon, S. Madbak, S. L. Whitbread and S. F. Lincoln, *Inorg. Chem.*, 1996, **35**, 2019.
6 A. K. W. Stephens, R. S. Dhillon, S. E. Madbak, S. L. Whitbread and S. F. Lincoln, *Inorg. Chem.*, 1996, **35**, 2019.
7 S. F. Lincoln, *Coord. Chem. Rev.*, 1997, **166**, 255.
8 J. Huskens and A. D. Sherry, *Chem. Commun.*, 1997, 845.
9 S. L. Whitbread, J. Weeks, P. Valente, M. A. Buntine, S. F. Lincoln and K. P. Wainwright, *Aust. J. Chem.*, 1997, **50**, 853; S. L. Whitbread, J. Weeks, P. Valente, M. A. Buntine, S. F. Lincoln and K. P. Wainwright, *Aust. J. Chem.*, 1999, **52**, 82.
10 R. Dhillon, S. F. Lincoln, S. Madbak, A. K. W. Stephens, K. P. Wainwright and S. L. Whitbread, *Inorg. Chem.*, 2000, **39**, 1855.
11 E. Cole, R. C. B. Copley, J. A. K. Howard, D. Parker, G. Ferguson, J. F. Gallagher, B. Kaitner, A. Harrison and L. Royale, *J. Chem. Soc.*, *Dalton Trans.*, 1994, 1619.
12 J. Huskens and A. D. Sherry, *J. Am. Chem. Soc.*, 1996, **118**, 4396.
13 J. Huskens and A. D. Sherry, *J. Chem. Soc.*, *Dalton Trans.*, 1998, 177.
14 P. D. Beer, P. K. Hopkins and J. D. McKinney, *Chem. Commun.*, 1999, 1253.
15 R. B. Lauffer, *Chem. Rev.*, 1987, **87**, 901.
16 J. F. Desreux and P. P. Barthelemy, *Nucl. Med. Biol.*, 1988, **15**, 9.
17 K. Micskei, L. Helm, E. Brücher and A. E. Merbach, *Inorg. Chem.*, 1993, **32**, 3844.
18 G. González, D. H. Powell, V. Tisières and A. E. Merbach, *J. Phys. Chem.*, 1994, **98**, 53.
19 V. Jaques and J. F. Desreux, *Inorg. Chem.*, 1994, **33**, 4048.
20 D. Parker, K. Pulukkody, F. C. Smith, A. Balsanov and J. A. K. Howard, *J. Chem. Soc.*, *Dalton Trans.*, 1994, 689.
21 R. S. Dhillon, S. E. Madbak, F. G. Ciccone, M. A. Buntine, S. F. Lincoln and K. P. Wainwright, *J. Am. Chem. Soc.*, 1997, **119**, 6126; R. S. Dhillon, S. E. Madbak, F. G. Ciccone, M. A. Buntine, S. F. Lincoln and K. P. Wainwright, *J. Am. Chem. Soc.*, 1998, **120**, 11212.
22 S. L. Whitbread, P. Valente, M. A. Buntine, P. Clements, S. F. Lincoln and K. P. Wainwright, *J. Am. Chem. Soc.*, 1998, **120**, 2862;

S. L. Whitbread, P. Valente, M. A. Buntine, P. Clements, S. F. Lincoln and K. P. Wainwright, *J. Am. Chem. Soc.*, 1998, **120**, 11212.
23 D. F. Shriver, P. W. Atkins and C. H. Langford, in *Inorganic Chemistry*, 2nd edn., Oxford University Press, Oxford, 1994, pp. 212–214.
24 S. F. Lincoln, *Prog. React. Kinet.*, 1977, **9**, 1.
25 Gaussian 94, Revision C.3, M. J. Frisch, G. W. Trucks, H. B. Schlegel, P. M. W. Gill, B. G. Johnson, M. A. Robb, J. R. Cheeseman, T. Keith, G. A. Petersson, J. A. Montgomery, K. Raghavachari, M. A. Al-Laham, V. G. Zakrzewski, J. V. Ortiz, J. B. Foresman, J. Cioslowski, B. B. Stefanov, A. Nanayakkara, M. Challacombe, C. Y. Peng, P. Y. Ayala, W. Chen, M. W. Wong, J. L. Andres, E. S. Replogle, R. Gomperts, R. L. Martin, D. J. Fox, J. S. Binkley, D. J. Defrees, J. Baker, J. P. Stewart, M. Head-Gordon, C. Gonzalez, J. A. Pople, Gaussian Inc., Pittsburgh, PA, 1995.
26 R. Yang and L. J. Zompa, *Inorg. Chem.*, 1976, **15**, 1499.
27 B. G. Cox, H. Schneider and J. J. Stroka, *J. Am. Chem. Soc.*, 1978, **100**, 4746.
28 (*a*) W. R. Wadt and P. J. Hay, *J. Chem. Phys.*, 1985, **82**, 284; (*b*) P. J. Hay and W. R. Wadt, *J. Chem. Phys.*, 1985, **82**, 299.
29 Programs used for X-ray analysis: TEXSAN, Structure Analysis Package, Molecular Structure Corporation, Houston, TX, 1992; C. K. Johnson, ORTEP II, Report ORNL-5136, Oak Ridge National Laboratory, Oak Ridge, TN, 1976.